HHS Public Access

Author manuscript

Kidney Int. Author manuscript; available in PMC 2020 February 01.

Published in final edited form as:

Kidney Int. 2019 February ; 95(2): 310–320. doi:10.1016/j.kint.2018.08.040.

Activation of Fibroblastic Reticular Cells in Kidney Lymph Node during Crescentic Glomerulonephritis

Vivek Kasinath, M.D.[#1,2], **Osman A. Yilmam, M.D.**[#1], **Mayuko Uehara, M.D.**[1], **Liwei Jiang, Ph.D.**[1], **Farideh Ordikhani, Ph.D.**[1], **Xiaofei Li, M.D.**[1], **David J. Salant, M.D.**[3], and **Reza Abdi, M.D.**[1,2,*]

[1]Transplantation Research Center, Boston University Medical Center, Boston, MA, USA

[2]Division of Renal Medicine, Brigham and Women's Hospital, Boston University Medical Center, Boston, MA, USA

[3]Renal Section, Boston University Medical Center, Boston, MA, USA

[#] These authors contributed equally to this work.

Abstract

Crescentic glomerulonephritis is an inflammatory condition characterized by rapid deterioration of kidney function. Previous studies of crescentic glomerulonephritis have focused on immune activation in the kidney. However, the role of fibroblastic reticular cells, which reside in the stromal compartment of the kidney lymph node, has not been studied in this condition. We investigated the activation of kidney lymph node-resident fibroblastic reticular cells in nephrotoxic serum nephritis, a classic murine model of crescentic glomerulonephritis. We found that increased deposition of extracellular matrix fibers by fibroblastic reticular cells in the kidney lymph node was associated with the propagation of high endothelial venules, specialized blood vessels through which lymphocytes enter the lymph node, as well as with expansion of the lymphatic vasculature. The kidney lymph node also contained an expanding population of pro-inflammatory T cells. Removal of the kidney lymph node, depletion of fibroblastic reticular cells, and treatment with anti-podoplanin antibody each resulted in reduction of kidney injury. Our findings suggest that modulating the activity of fibroblastic reticular cells may be a novel therapeutic approach in crescentic glomerulonephritis.

Graphical Abstract

[*]Corresponding author: Reza Abdi, M.D., Brigham and Women's Hospital Transplantation Research Center, 221 Longwood Ave., 3rd Floor, Boston, MA 02115, Fax: 617-732-5254, Phone: 617-732-7249, rabdi@rics.bwh.harvard.edu.

Disclosure

The authors declare no competing financial interests.

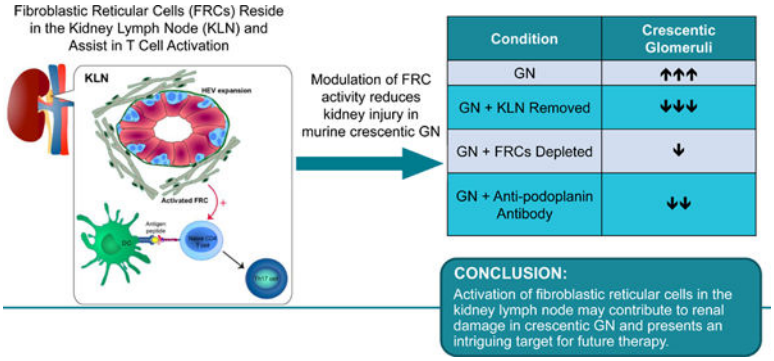

Keywords

Acute kidney injury; anti-GBM disease; glomerulonephritis; lymphocyte; Goodpasture's syndrome

Introduction

Crescentic glomerulonephritis (GN) is a rapidly progressive inflammatory condition affecting the kidneys that can lead to renal failure in humans within days.[1,2] If left untreated, the majority of patients with crescentic GN will die or become dialysis-dependent within six months.[3] The central role of $CD4^+$ T cell-mediated renal injury in nephrotoxic serum nephritis (NTN), a classic experimental anti-glomerular basement membrane (anti-GBM) antibody-mediated model of crescentic GN, has been well established.[4–10]

Several previous studies have elucidated the role of fibroblastic reticular cells (FRCs), the prominent cells that comprise the stromal compartment of the lymph node (LN), in the activation of an immune response.[11–18] FRCs express the membrane glycoprotein podoplanin (PDPN), but they do not express the leukocyte marker CD45 or the vascular marker CD31, a unique cellular signature in the LN.[15] FRCs secrete the chemokines CCL19, CCL21, and CXCL12, which promote the trafficking of naïve T cells into the LN through specialized vasculature known as high endothelial venules (HEVs).[14] FRCs also maintain the integrity of HEVs through interactions between PDPN on the FRCs and C-type lectin-like receptor 2 (CLEC-2) on platelets.[19] The chemokines secreted by FRCs contain the newly arrived T cells within the paracortex (T cell zone) of the LN, where the FRCs provide conduits upon which these naïve T cells and antigen-presenting cells migrate and interact, resulting in activation of the T cells.[14]

Though the kidney has been proven to be a site of recruitment for activated $CD4^+$ Th1 and Th17 cells via expression of chemokines such as CCL20 and CXCL9,[10] the role of the kidney lymph node (KLN) as a secondary lymphoid organ where these T cells are also activated in NTN has not yet been explored in depth.[20] $CD4^+$ T cells are activated in the spleen during NTN,[10] but splenectomy does not affect kidney damage significantly in these mice.[21] This finding raises the hypothesis that the KLN may be the key secondary lymphoid organ responsible for propagation of the immune response in NTN. The objectives of this study are to explore the phenotypic changes that occur to FRCs in the KLN during the early

stages of the immune response and examine the effects that modulation of the activity of FRCs has on kidney damage in NTN.

Results

Microarchitectural compartmentalization in KLN reflects activation of cell-mediated immune response by FRCs

We investigated crescentic GN using the classic accelerated NTN mouse model. Hematoxylin and eosin (H&E)-stained kidney tissue revealed cellular crescent formation in the glomeruli by NTN Day 7 (Figure S1). $CD3^+$ T **cell** and $F4/80^+$ macrophage infiltrates **in** the kidney also rose significantly during the early course of the disease (Figure S2). The blood urea nitrogen (BUN), a serologic marker of kidney injury, peaked at NTN Day 2 but remained significantly elevated at Day 7 (Figure S3). Next, we established that the KLN receives lymphatic flow from the kidney by injecting a bolus of India ink into the lymphatic vessel that drains the kidney (Figure S4). Review of H&E staining of the KLN at different time points in the course of NTN revealed that the size of the paracortex increased, which marginalized the follicles in the cortex to the periphery progressively through Days 2 and 7 (Figure 1A). The total cell count in the KLN also increased significantly at Day 7 (Figure S5).

We compared the microarchitecture in the KLN between the control mice and NTN mice at Day 2 via immunofluorescence staining (Figure 1B). $PDPN^+$ cells were distributed uniformly throughout the KLN in the control mice. However, $PDPN^+$ cells in the NTN **mice** were organized into a lattice-like pattern. Next, we examined ER-$TR7^+$ staining to assess the creation of extracellular matrix (ECM) fibers by FRCs, as they secrete an antigen recognized by the ER-TR7 antibody in the reticular network that they produce.[16] PDPN and the ER-TR7 antigen colocalized throughout the control KLN. However, ER-TR7 stained just a portion of the NTN Day 2 KLN, and the expression of the ER-TR7 antigen was lost in the other portion. The ER-$TR7^+$ compartment also colocalized with laminin, a marker of the basal lamina. Laminin fibers were thicker in the ER-$TR7^+$ area and less dense in the area of lower ER-$TR7^+$ staining, reflecting the presence of the ER-TR7 antigen in the ECM and demonstrating ECM fiber production by FRCs.

Examination of $LYVE1^+$ lymphatic endothelial cells revealed evidence of thickening and branching of new lymphatic vessels in the KLN by Day 2, and the location of these vessels coincided with the area of ECM production by FRCs (Figure 1B). HEVs were also marginalized at Day 2 by an expanding T cell zone in the KLN (Figure 1C). The $PDPN^+$ FRCs located in the T cell zone produced laminin fibers of decreased density, and the ER-TR7 antigen was essentially absent in this area (Figure 1B).

Close inspection of the HEVs at Day 2 revealed a more organized support structure composed of ER-$TR7^+$ FRCs surrounding the HEV in comparison to the control KLN (Figure 1D).

This microarchitectural compartmentalization associated with a dual phenotype of FRCs—ECM fiber-secreting in the vascul ature compartment and non-fiber secreting in the T cell zone—continued at NTN Day 7 (Figure 2A).

We also quantified cell populations of the KLN by flow cytometry, which revealed progressive increases in FRCs as a percentage of all KLN cells through Day 7 (Figure 2B). The percentage of the HEV-specific peripheral node addressin $(PNAd)^+$ endothelial cells also increased through Day 7 (Figure 2C). Representative flow cytometry plots for the FRCs and $PNAd^+$ cells in the KLN are provided (Figure 2D). Recruitment of T cells to the LN is one of the key functions of FRCs. We found that the gene expression of the chemokines CCL19 and CCL21 increased significantly in the KLN at Day 2 (Figure 2E). The increase in these FRC-produced chemokines was associated with increased trafficking of T cells, as demonstrated by expanded populations of $CD4^+$ effector memory T cells ($CD4^+CD44^{high}CD62L^{low}$) and Th17 ($CD4^+IL\text{-}17A^+$) cells in the KLN through Days and 7 of the disease course in comparison to control (Figure 2F-G). Representative flow cytometry plots for the Th17 cells in the KLN are provided (Figure 2H).

H&E staining of non-draining lymph nodes revealed no significant change in size or appearance during the disease course (Figure S6). In addition, no significant increase in the $CD4^+$ effector memory cell population ($CD4^+CD44^{high}CD62L^{low}$) of the non-draining lymph node or spleen was observed at Day 2 (Figure S7).

KLN removal results in amelioration of kidney injury in NTN

To investigate the importance of the KLN to the pathogenesis of NTN, we removed the KLNs from mice that we subjected subsequently to NTN (Figure 3). The kidneys of mice that underwent bilateral KLN removal had a significantly lower percentage of crescentic glomeruli at Day 7, in comparison to the control mice that underwent sham surgery without removal of the KLNs (Figure 3A-B). The infiltration of $CD3^+$ T cells and $F4/80^+$ macrophages in the kidneys of mice from which the KLNs were removed was also significantly lower than the control group (Figure 3C-D). Finally, the KLN removed group also had lower BUNs at Days 2 and 7 (Figure 3E).

To identify the specific contribution of the FRCs in the KLN to the immune response in NTN, we induced NTN in a group of mice that were not pre-immunized with sheep IgG. Five days prior to the induction of NTN, the KLNs were removed surgically from half of these mice, while the other half underwent sham surgery and were designated as the control group. Glomerular crescents formed in these mice at NTN Week 3. However, the kidneys from the mice that underwent bilateral removal of KLNs had a significantly lower percentage of crescentic glomeruli at Week 3 than the kidneys from the control mice (Figure 3F-G). This reduction in crescentic glomeruli was accompanied by less severe infiltration of the kidneys by $F4/80^+$ macrophages (Figure 3H-I).

Finally, the systemic humoral immune response against sheep IgG was compared between the non-immunized NTN mice that underwent sham surgery and those that underwent KLN removal by ELISA of the sera at Week 3. No significant difference in mouse anti-sheep IgG antibody levels was found between these two groups (Figure S8).

FRC depletion reproduces protective effect of KLN removal on kidney injury in NTN

Next, we examined the effect of FRC depletion on NTN through the use of *CCl19*-Cre x *Rosa-26*-diphtheria toxin receptor (CCL19-Cre x iDTR) mice, a transgenic mouse strain from a C57Bl/6 background, in which the FRCs express diphtheria toxin (DT) receptor (Figure 4). First, we established that the administration of DT depleted the FRCs in the KLNs of these mice (Figure S9). We found that the glomeruli in the kidneys of these mice developed fewer crescents, in comparison to the C57Bl/6 control mice, also treated with DT (Figure 4A-B). The BUN of the CCL19-Cre x iDTR mice was significantly lower than the control mice at Day 7 (Figure 4C). Infiltration of $CD3^+$ T cells and $F4/80^+$ macrophages decreased in the kidneys of CCL19-Cre x iDTR mice, in comparison to the control group (Figure 4D-E).

FRC depletion also reduced the density of the ER-$TR7^+$ and laminin fibers in the KLN, inhibiting the expansion of the lymphatic endothelium robustly (Figure 4F). Close observation of HEVs also revealed reduced pocket formation, representative of decreased developmental complexity of these vessels following FRC depletion (Figure 4G). This hindrance in HEV development was associated with **a** significant decrease in the population of $CD4^+$ effector memory cells ($CD4^+CD44^{high}CD62L^{low}$) and a reduction of Th17 cells ($CD4^+$IL-$17A^+$) in the KLN following FRC depletion (Figure 4H).

Treatment with anti-PDPN antibody results in improvement of NTN

We next examined the effect of treatment with an anti-PDPN antibody (anti-PDPN) on kidney injury (Figure 5). The effect of this antibody on *in vivo* activity of FRCs remains to be determined. H&E staining of the kidney at Day 7 revealed a lower percentage of crescentic glomeruli in comparison to the control mice that received the Syrian Hamster IgG isotype control antibody (Figure 5A-B). BUN at Day 2 was significantly lower in the anti-PDPN treated mice, in comparison to the control group (Figure 5C). The infiltration of $F4/80^+$ macrophages in the kidney was reduced significantly following anti-PDPN treatment (Figure 5D-E).

Immunohistochemistry of the KLNs of the anti-PDPN group at Day 2 demonstrated an obscuration of the typical lattice-like pattern of $PDPN^+$ cells, which was otherwise noted to be present at this stage of the disease and seen in the KLN of the mice treated with the isotype control (Figure 5F). In addition, deposition of laminin fibers was less organized in the anti-PDPN group (Figure 5F). $LYVE1^+$ staining revealed a corresponding decrease in expansion of the lymphatic vessels (Figure 5F). The $CD3^+$ T cell zone was also decreased (Figure 5G).

Flow cytometric analysis of the cells in the KLN revealed significantly decreased $CD4^+$ effector memory cell ($CD4^+CD44^{high}CD62L^{low}$) and Th17 cell ($CD4^+$IL-$17A^+$) populations at Day 2 in the KLNs from the mice treated with anti-PDPN versus the isotype control antibody (Figure 5H).

Discussion

A lymphatic duct connects the kidney directly to the KLN in the mouse, an anatomical placement that designates the KLN as the sentinel lymph node where antigens from the kidney are carried by the lymph. This location primes the KLN as an ideal site for the earliest detection of injurious events in the kidney. A previous study demonstrated that the amelioration of kidney injury in NTN is accompanied by an increase in the percentage of $CD4^+FoxP3^+$ regulatory T cells in the KLN following transfusion of immunoregulatory $CD206^+$ M2 macrophages.[22] However, our study is the first to focus specifically on the association between the pro-inflammatory activity of FRCs in the KLN and kidney damage in crescentic GN.

FRCs are cells of mesenchymal origin that can adopt a pro-inflammatory phenotype, primarily by creating a reticular network on which incoming antigen-presenting cells can migrate, assisted by secretion of chemokines such as CCL19 and CCL21, and present antigens to naïve $CD4^+$ T cells.11–16 In this study, we demonstrated the deposition of ECM fibers along tracks that correspond with the location of FRCs in the KLN at NTN Day 2. FRCs deposited ECM fibers around the expanding HEVs during the initiation of the immune response in the KLN. This maintenance of HEVs ensures the proper influx of T cells into the LN.[19] Interestingly, the HEVs located at the frontier of the expanding T cell zone, closest to the expanding lymphatic vessels, appeared to be most elongated in the KLN. This elongation likely reflects the role of these HEVs in providing the greatest surface area through which the naïve T cells could cross into the lymph node.

We have also demonstrated that the lymphatic vasculature organizes and expands around the area of ECM fiber deposition by FRCs. This expansion may allow for optimal crosstalk between antigen-presenting cells arriving from the kidney and effector T cells leaving the LN.

The importance of Th17 cells to the pathogenesis of NTN has been proven in previous studies.[5,10,23–25] We demonstrated increased expression of the FRC-produced chemokines CCL19 and CCL21 in the KLN, which can lead to increased trafficking of naïve T cells from the vasculature to the KLN and explain the expanded population of Th17 cells we observed in the KLN, starting at Day 2.This rise precedes their peak in the kidney by a number of days.[10]

Removal of the KLN resulted in reduction of renal injury, suggesting its importance to the propagation of the immune response in NTN. The nephritogenic sheep IgG antigen from the kidney may reach the KLN via passage through the lymph or transport by kidney-resident dendritic cells, which would facilitate the activation of T cells in the KLN, aided by the activity of FRCs. However, KLN removal was not associated with a reduction in anti-sheep IgG antibodies, which demonstrates that NTN is marked substantially by a systemic immune response. Previous studies have demonstrated that $CD4^+$ T cells are activated in the spleen during NTN,[10] but splenectomy does not affect renal damage.[21] Future studies should investigate the effects of the absence of other lymphoid tissues on the course of NTN. These experiments apply directly to the accelerated NTN model, in which initial immune activation

occurs most likely in the skin-draining LNs. In addition, observation of microarchitectural changes, as well as activation, expansion, and differentiation of $CD4^+$ T cells in these LNs would be interesting. Furthermore, the direct effect of sheep IgG on the differentiation of $CD4^+$ T cells into Th17 cells in the KLN should be investigated in future studies.

Depletion of FRCs **in** the CCL19-Cre x iDTR mice resulted in protection from renal injury by decreasing the activation of $CD4^+$ T cells in the **LN.** These findings resembled those from a previous anti-viral immunity study, in which FRC depletion resulted in reduction of activated T cells in the lymph node following infection by influenza A virus.[26] One potential drawback associated with using the CCL19-Cre x IDTR model is that the administration of DT to these mice can ablate all cells that express CCL19, including cells in the trachea, colon, and even some podocytes in the kidney during pro-inflammatory conditions.[27] However, the acuity of our disease model likely prevented significant depletion of CCL19-expressing cells in other organs.

We explored further the effects of the activity of FRCs on the immune response in NTN by treating mice with anti-PDPN. The role of anti-PDPN antibodies as a therapy for malignancy and thrombosis has been explored previously,[28,29] but their therapeutic effect on *in vivo* animal models of immune-mediated human diseases has never been investigated. The development of targeted anti-inflammatory therapy for crescentic GN is an urgent unmet clinical need, as current therapeutic modalities consist of systemic immunosuppressive medications with critical off-target toxicity on sites such as the bone marrow, which can lead to severe infection and death. Similar to the effect of FRC depletion, we found that treatment with anti-PDPN ameliorated kidney injury in NTN by decreasing T cell activation in the LN. Anti-PDPN treatment led to disorganization of laminin fibers in the KLN, which was associated with remarkably reduced expansion of the lymphatic vasculature. Therefore, we hypothesize that anti-PDPN treatment inhibits the constitutive ECM fiber-secreting properties of FRCs, though the mechanism behind this effect is unclear and represents an intriguing future topic for investigation. Hence, directing immunosuppressive therapy against FRCs represents a novel modality in the treatment of crescentic GN and immune-mediated diseases in general.

We have confirmed that FRCs are fundamental to the propagation of the immune response in NTN. Our findings open the door to the pursuit of therapies directed towards modulation of the activity of the FRCs in the LN that would create a promising new frontier in the treatment of immune-mediated diseases.

Methods

Please refer to supplemental material for complete Methods.

Animals

Male CD-1® IGS mice (Charles River Laboratories, Shrewsbury, MA) were used in all experiments, except for those involving CCL19-Cre x iDTR mice, which contain a background of C57Bl/6, and for which C57Bl/6J mice (Jackson Laboratory, Bar Harbor, ME) were used as controls.

Induction of Accelerated NTN model

The accelerated NTN model was induced in 8–10 week old mice as per the classic protocol,[30,31] using nephrotoxic serum (NTS) prepared from sheep immunized against Sprague-Dawley rat glomeruli, as described.[32] Mice were sensitized via subcutaneous injection of sheep IgG (Thermo Fisher Scientific, Rockford, IL) emulsified in Complete Freund's Adjuvant (Sigma-Aldrich, St. Louis, MO) to several different sites on the back (200 μg of sheep IgG for CD-1® IGS mice and 1 mg for CCL19-Cre x iDTR and C57/Bl6j mice). Five days later, the NTN mice received three consecutive daily intravenous injections of sheep nephrotoxic serum (NTS) (0.067 g/mL) (50 μL for CD-1 mice and 100 μL for CCL19-Cre x iDTR and C57/Bl6j mice), and the negative control mice received an equivalent amount of normal sheep serum (NSS) (abcam, Cambridge, MA).

One group comprised of 5 mice that received NTS and 4 mice that received NSS was sacrificed 2 days following the initial injection of serum (Day 2). Another group of 6 mice (3 mice that received NTS and 3 that received NSS) was sacrificed at Day 7.

A randomized subset of 4 mice underwent surgical removal of the KLNs on the day of sensitization, 5 days prior to injection of NTS. A corresponding group of 5 mice underwent sham surgery (without removal of KLNs) and was used as control for these mice.

In addition, a group of 16 mice was randomized to undergo either bilateral KLN removal (8 mice) or sham surgery (8 mice), in the absence of sensitization with sheep IgG, 5 days prior to injection of NTS. 8 of the mice (4 from each group) were sacrificed at Day 3, and the other 8 mice were sacrificed at Week 3.

FRC Depletion

NTN was induced as above in a group of 5 *CCL19*-Cre x iDTR mice (received courtesy of Shannon Turley, Genentech, South San Francisco, CA) and in 4 corresponding control C57Bl/6J mice (Jackson Laboratory). All mice received intraperitoneal injections of diphtheria toxin from *Corynebacterium diphtheriae* (DT) (Sigma-Aldrich) 30 ng daily for three days, starting two days prior to the first injection of NTS (Days −2, −1, and 0). They were injected again with DT 30 ng on Day 4. The mice were sacrificed on Day 7.

Anti-PDPN Antibody Treatment

CD-1® IGS mice (Charles River Laboratories) were randomized to two groups, and NTN was induced in all mice, as above. The treatment group of 5 mice received injections of anti-PDPN antibody (BioLegend, Clone 8.1.1, Cat#127402) 33.3 μg each on Days 1, 3, and 5, for blockade of the molecular function of PDPN on FRCs. The control group of 3 mice received injections of LEAF™ Purified Syrian Hamster isotype control antibody (Biolegend, clone SHG-1, Cat#402002) 33.3 μg each on the same schedule. The mice were sacrificed on Day 7. The experiment was then repeated with sacrifice at Day 2.

Serologic Studies of Renal Damage

Blood was obtained from the tail veins of mice at Days 0, 2, and 7, or brachial artery at time of sacrifice, for measurement of BUN using Infinity Urea (Thermo Fisher Scientific, Middletown, VA).

Extraction of Leukocytes from Lymph Nodes and Spleen

The KLNs, non-draining LNs, and spleens of the mice were harvested and digested into single cell suspensions at the time of sacrifice for subsequent experiments.

Flow Cytometry

The single cell suspensions above were divided into samples that underwent intracellular cytokine staining and those that underwent surface and intracellular non-cytokine antibody staining. The cells that underwent intracellular cytokine staining were first incubated with phorbol 12-mystirate 13-acetate (PMA) (100 ng/mL) (Sigma-Aldrich, St. Louis, MO), ionomycin (1 μg/mL) (Sigma-Aldrich), and GolgiStop™ protein transport inhibitor (BD Biosciences, San Jose, CA) at 37°C for 4 hr., prior to staining for viabil ity and surface markers.

Flow cytometry was performed via BD FACSCanto™ II flow cytometer (BD Biosciences). Analysis of flow cytometry results was performed via FlowJo software (FlowJo LLC, Ashland, OR).

Immunohistochemistry of Kidneys and KLNs

Immunofluorescence staining of the kidney and KLNs was performed on frozen sections obtained at the time of sacrifice. The sections were visualized using the microscope Evos FL Auto 2 by Invitrogen (ThermoFisher Scientific).

Histologic Analysis of Kidney Injury and Immune Cell Infiltration

Ten random fields from the cortex of each kidney, stained with hematoxylin & eosin (H&E), were assessed blindly at 400x magnification. The total number of glomeruli was counted, and the number of glomeruli with crescents was recorded.

$CD3^+$ cells and $F4/80^+$ cells were counted in five pictures of kidneys per group taken at 200x and 400x magnification by the Evos FL Auto 2 microscope.

Assessment of Gene Expression by RT-PCR

RNA was isolated with TRIzol® (ThermoFIsher Scientific), first strand of cDNA was synthesized using 2 μg of RNA and High-Capacity Reverse Transcriptase (ThermoFisher Scientific), and RT-PCR was performed using SYBR® Green PCR reagents (Bio-Rad, Hercules, CA), with normalization of RNA levels against GAPDH.

Measurement of Mouse Anti-Sheep IgG by ELISA

Mouse anti-sheep IgG antibody (IgG2b) levels in the sera of 4 non-immunized NTN Week 3 mice that underwent sham surgery and 4 non-immunized NTN Week 3 mice that underwent

KLN removal were measured by ELISA. The corresponding antibody levels in 3 non-immunized mice that received normal sheep serum were used as a control group.

Statistics

Statistical analysis of all data obtained in these experiments was performed via Prism 5 (GraphPad Software, Inc., La Jolla, CA). The Wilcoxon rank sum test was performed to assess the statistical differences between two groups, and 1-way non-parametric analysis of variance was used to assess the statistical differences between three groups for significance. Data are presented in the figure legends as sample size, mean ± standard error of mean (SEM), range, and median.

Supplementary Material

Refer to Web version on PubMed Central for supplementary material.

Acknowledgments

The authors would like to thank Dr. Yarong Sunny Lu (InvivoEx, Allston, MA) for cutting and staining tissue with H&E for all experiments.

This work was supported by the NIH [T32DK007527 (V.K.), RO1DK0900029 (D.J.S) and R01AI126596 (R.A.)].

References

1. Piyaphanee N, Ananboontarick C, Supavekin S, et al. Renal outcomes and risk factors for ESRD in children with rapidly progressive glomerulonephritis. Pediatr Int 8 20 2016.
2. Andres G, Brentjens J, Kohli R, et al. Histology of human tubulo-interstitial nephritis associated with antibodies to renal basement membranes. Kidney Int 6 1978;13(6):480–491. [PubMed: 362036]
3. Wilson CB, Dixon FJ. Anti-glomerular basement membrane antibody-induced glomerulonephritis. Kidney Int 2 1973;3(2):74–89. [PubMed: 4571918]
4. Tipping PG, Holdsworth SR. T cells in crescentic glomerulonephritis. J Am Soc Nephrol 5 2006;17(5):1253–1263. [PubMed: 16624930]
5. Paust HJ, Turner JE, Steinmetz OM, et al. The IL-23/Th17 axis contributes to renal injury in experimental glomerulonephritis. J Am Soc Nephrol 5 2009;20(5):969–979. [PubMed: 19339380]
6. Lloyd CM, Dorf ME, Proudfoot A, et al. Role of MCP-1 and RANTES in inflammation and progression to fibrosis during murine crescentic nephritis. J Leukoc Biol 11 1997;62(5):676–680. [PubMed: 9365123]
7. Paust HJ, Ostmann A, Erhardt A, et al. Regulatory T cells control the Th1 immune response in murine crescentic glomerulonephritis. Kidney Int. Jul 2011;80(2):154–164.
8. Paust HJ, Riedel JH, Krebs CF, et al. CXCR3+ Regulatory T Cells Control TH1 Responses in Crescentic GN. J Am Soc Nephrol 7 2016;27(7):1933–1942. [PubMed: 26534920]
9. Turner JE, Krebs C, Tittel AP, et al. IL-17A production by renal gammadelta T cells promotes kidney injury in crescentic GN. J Am Soc Nephrol 9 2012;23(9):1486–1495. [PubMed: 22797181]
10. Paust HJ, Turner JE, Riedel JH, et al. Chemokines play a critical role in the cross-regulation of Th1 and Th17 immune responses in murine crescentic glomerulonephritis. Kidney Int 7 2012;82(1): 72–83. [PubMed: 22495297]
11. Acton SE, Farrugia AJ, Astarita JL, et al. Dendritic cells control fibroblastic reticular network tension and lymph node expansion. Nature 10 23 2014;514(7523):498–502. [PubMed: 25341788]
12. Alvarenga HG, Marti L. Multifunctional roles of reticular fibroblastic cells: more than meets the eye? J Immunol Res 2014;2014:402038. [PubMed: 24829927]

13. Astarita JL, Cremasco V, Fu J, et al. The CLEC-2-podoplanin axis controls the contractility of fibroblastic reticular cells and lymph node microarchitecture. Nat Immunol 1 2015;16(1):75–84. [PubMed: 25347465]
14. Brown FD, Turley SJ. Fibroblastic reticular cells: organization and regulation of the T lymphocyte life cycle. J Immunol 2 15 2015;194(4):1389–1394. [PubMed: 25663676]
15. Fletcher AL, Acton SE, Knoblich K. Lymph node fibroblastic reticular cells in health and disease. Nature Rev Immunol 6 2015;15(6):350–361. [PubMed: 25998961]
16. Katakai T, Hara T, Sugai M, et al. Lymph node fibroblastic reticular cells construct the stromal reticulum via contact with lymphocytes. J Exp Med 9 20 2004;200(6):783–795. [PubMed: 15381731]
17. Pasztoi M, Pezoldt J, Huehn J. Microenvironment Matters: Unique Conditions Within Gut-Draining Lymph Nodes Favor Efficient De Novo Induction of Regulatory T Cells. Prog Mol Biol Transl Sci 2015;136:35–56. [PubMed: 26615091]
18. Siegert S, Huang HY, Yang CY, et al. Fibroblastic reticular cells from lymph nodes attenuate T cell expansion by producing nitric oxide. PLoS One 2011;6(11):e27618. [PubMed: 22110693]
19. Herzog BH, Fu J, Wilson SJ, et al. Podoplanin maintains high endothelial venule integrity by interacting with platelet CLEC-2. Nature 10 3 2013;502(7469):105–109. [PubMed: 23995678]
20. Artinger K, Kirsch AH, Aringer I, et al. Innate and adaptive immunity in experimental glomerulonephritis: a pathfinder tale. Pediatr Nephrol 5 11 2016.
21. Artinger K, Kirsch AH, Aringer I, et al. The Spleen Plays No Role in Nephrotoxic Serum Nephritis, but Constitutes a Place of Compensatory Haematopoiesis. PLoS One 2015;10(8):e0135087. [PubMed: 26247770]
22. Du Q, Tsuboi N, Shi Y, et al. Transfusion of CD206+ M2 Macrophages Ameliorates Antibody-Mediated Glomerulonephritis in Mice. Am J Pathol 12 2016;186(12):3176–3188. [PubMed: 27855848]
23. Krebs CF, Turner JE, Paust HJ, et al. Plasticity of Th17 Cells in Autoimmune Kidney Diseases. J Immunol 7 15 2016;197(2):449–457. [PubMed: 27271566]
24. Ooi JD, Phoon RK, Holdsworth SR, et al. IL-23, not IL-12, directs autoimmunity to the Goodpasture antigen. J Am Soc Nephrol 5 2009;20(5):980–989. [PubMed: 19357249]
25. Krebs CF, Kapffer S, Paust HJ, et al. MicroRNA-155 drives TH17 immune response and tissue injury in experimental crescentic GN. J Am Soc Nephrol 12 2013;24(12):1955–1965. [PubMed: 23949802]
26. Cremasco V, Woodruff MC, Onder L, et al. B cell homeostasis and follicle confines are governed by fibroblastic reticular cells. Nat Immunol 10 2014;15(10):973–981. [PubMed: 25151489]
27. Valino-Rivas L, Gonzalez-Lafuente L, Sanz AB, et al. Non-canonical NFkappaB activation promotes chemokine expression in podocytes. Sci Rep 6 29 2016;6:28857. [PubMed: 27353019]
28. Abe S, Kaneko MK, Tsuchihashi Y, et al. Antitumor effect of novel anti-podoplanin antibody NZ-12 against malignant pleural mesothelioma in an orthotopic xenograft model. Cancer Sci 9 2016;107(9):1198–1205. [PubMed: 27294401]
29. Payne H, Ponomaryov T, Watson SP, et al. Mice with a deficiency in CLEC-2 are protected against deep vein thrombosis. Blood 4 6 2017;129(14):2013–2020. [PubMed: 28104688]
30. Lloyd CM, Minto AW, Dorf ME, et al. RANTES and monocyte chemoattractant protein-1 (MCP-1) play an important role in the inflammatory phase of crescentic nephritis, but only MCP-1 is involved in crescent formation and interstitial fibrosis. J Exp Med 4 07 1997;185(7):1371–1380. [PubMed: 9104823]
31. Topham PS, Csizmadia V, Soler D, et al. Lack of chemokine receptor CCR1 enhances Th1 responses and glomerular injury during nephrotoxic nephritis. J Clin Invest 12 1999;104(11): 1549–1557. [PubMed: 10587518]
32. Salant DJ, Cybulsky AV. Experimental glomerulonephritis. Methods Enzymol 1988;162:421–461. [PubMed: 3265756]

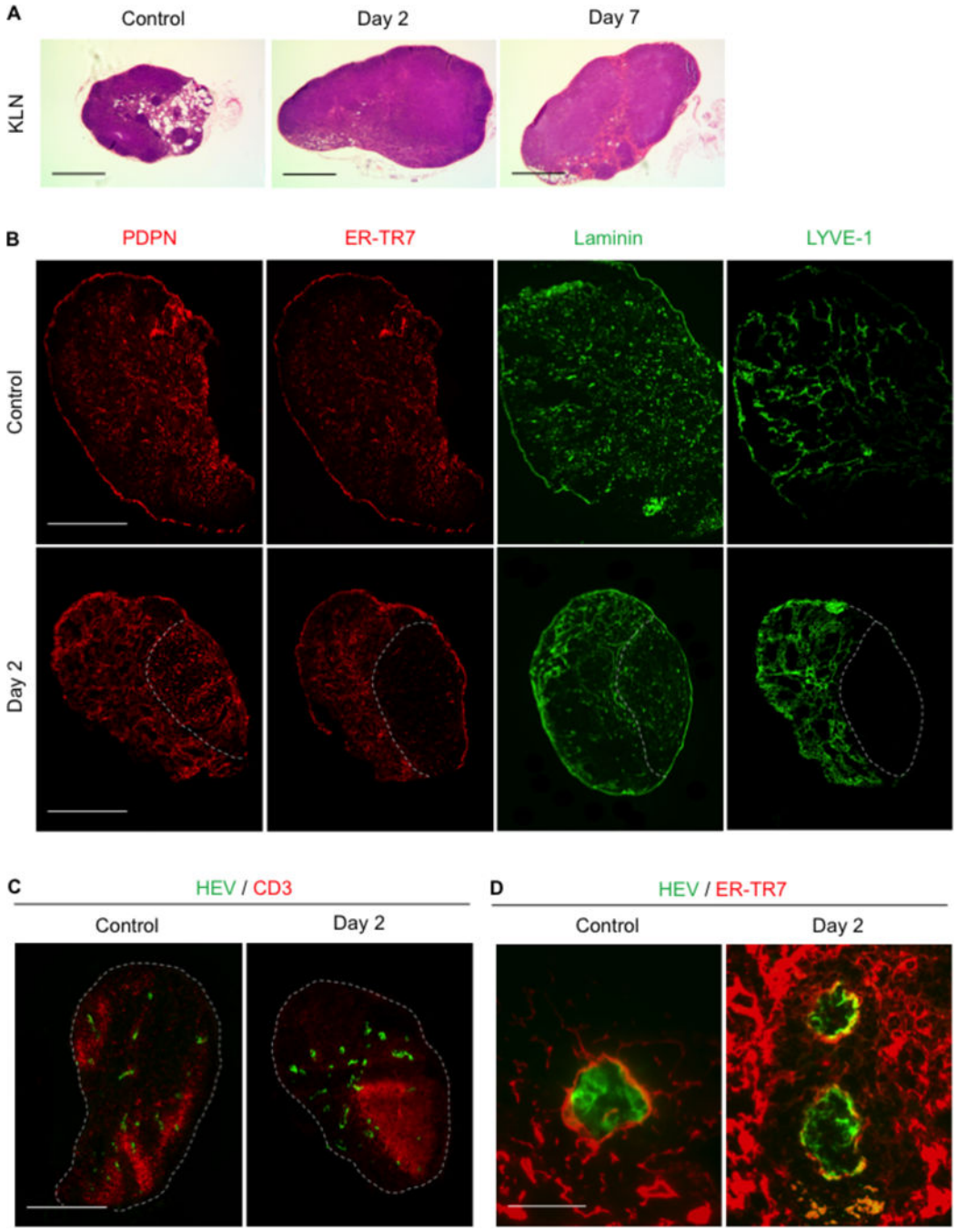

Figure 1. Microarchitecture changes in KLN during NTN.

(**A**) H&E stains of KLN reveal progressively increasing size and cell density of paracortex through Days 2 and 7. Scale bar 500 μm. (**B**) PDPN^{+} cells (red) remain uniformly distributed but form lattice-like structure at Day 2. ER-TR7^{+} (red) staining reveals loss of expression in one portion of the lymph node, correlating with area of reduced density of laminin (green) fibers at Day 2. Lymphatic endothelial cell marker LYVE1^{+} (green) staining at Day 2 reveals thickened lymph vessels in area of increased ER-TR7^{+} expression and laminin density. Scale bar 500 μm.(**C**) CD3^{+} T cell zone (red) displaces PNAd^{+} HEVs

(green) and corresponds to area of decreased ER-TR7 and laminin secretion at Day 2. Scale bar 500 μm.(**D**) $PNAd^+$ HEVs (green) in Day 2 KLN are surrounded by a network of thickened ER-$TR7^+$ fibers (red) in comparison to control KLN. Scale bar 50 μm. KLN: kidney lymph node, NTN: nephrotoxic serum nephritis, H&E: hematoxylin and eosin, PDPN: podoplanin, PNAd: peripheral node addressin, HEVs: high endothelial venules.

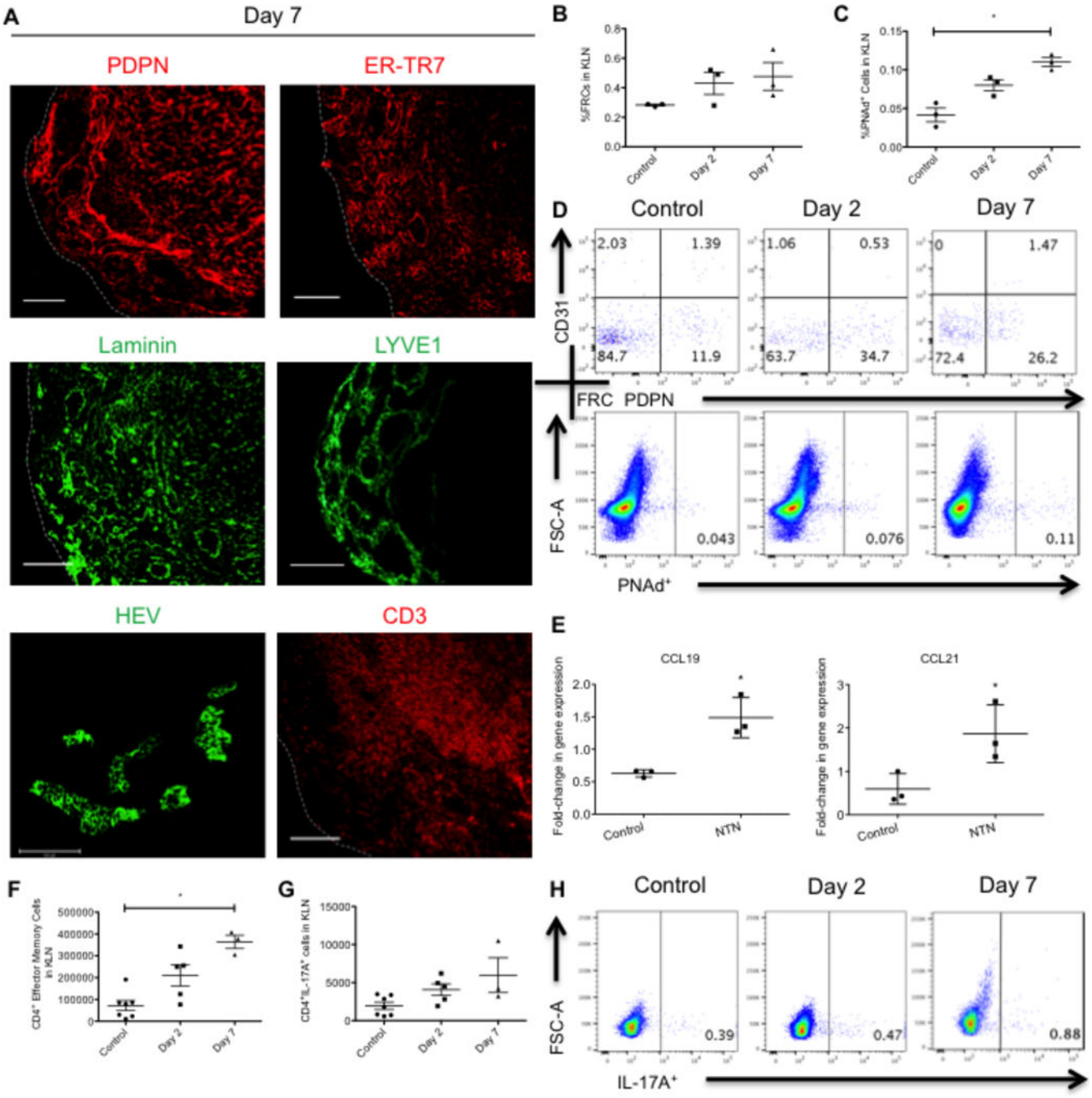

Figure 2. Microarchitectural changes in KLN persist at NTN Day 7.

(A) Staining of PDPN (red), ER-TR7 (red), laminin (green), and LYVE1 (green) display persistent marginalization by expanding $CD3^+$ T cell zone (red) at NTN Day 7, while elongated $PNAd^+$ HEVs (green) demonstrate signs of activation. Scale bars 200 μm for PDPN, ER-TR7, laminin, LYVE-1 and CD3, 100 μm for HEV. (**B**) $CD31^-PDPN^+$ FRCs as percentage of all cells in KLN increase at Days 2 (n=3, mean 0.43%±0.0755, range 0.28–0.52%, median 0.49%) and 7 (n=3, 0.4767%±0.09387, 0.35–0.66%, median 0.42%) in comparison to control (n=3, 0.2833%±0.006667, 0.27–0.29%, median 0.29%), as

determined by flow cytometry (p=0.1741). (**C**) The percentage of $PNAd^+$ cells also increases at Days 2 (n=3, 0.08%±0.007211, 0.066–0.090%, median 0.084%) and 7 (n=3, 0.11%±0.005774, 0.10–0.12%, median 0.11%), in comparison to control (n=3, 0.04167% ±0.00895, 0.026–0.057%, median 0.042%). **(D)** Representative flow cytometry plots for $CD31^-PDPN^+$ FRCs (gated under $CD45^-$ cells) and $PNAd^+$ cells (gated under live cells) in the KLN. **(E)** Gene expression of FRC-produced chemokines CCL19 and CCL21 in KLN increase at Day 2 in comparison to control (CCL19: Control: n=3, 0.6279±0.03237, 0.563207–0.662933, median 0.657491; NTN: n=3, 1.488±0.1786, 1.270867–1.842077, median 1.350268) (CCL21: Control: n=3, 0.5952±0.2036, 0.355335–1, median 0.430177; NTN: n=3,1.867±0.3841, 1.341689–2.614839, median 1.643603). (**F**) $CD4^+$ effector memory cell population ($CD4^+CD44^{high}CD62L^{low}$) in KLN peaks at Day 7 (Control: n=7,72046±23124, 10962.6–190960, median 79000; Day 2: n=5, 209760±48115,76877–342684, median 249600; Day 7: n=3, 363906±30531, 305340–408156,median 378222). (**G**) Th17 cell population ($CD4^+IL\text{-}17A^+$) in KLN peaks at Day 7 (Control: n=7, 1949±483.9, 584–3478, median 1800; Day 2: n=5, 4070±763, 1922–4928, median 4477; Day 7: n=3, mean 5976±2278, 3231–10497, median 4200) (p=0.0632). (H) Representative flow cytometry plots for Th17 cells in the KLN (gated under $CD4^+$ cells). *p<0.05. KLN: kidney lymph node, NTN: nephrotoxic serum nephritis, PNAd: peripheral node addressin, HEVs: high endothelial venules, FRCs: fibroblastic reticular cells. Data in graphs are presented as means (horizontal bar) ± SEM (vertical bars).

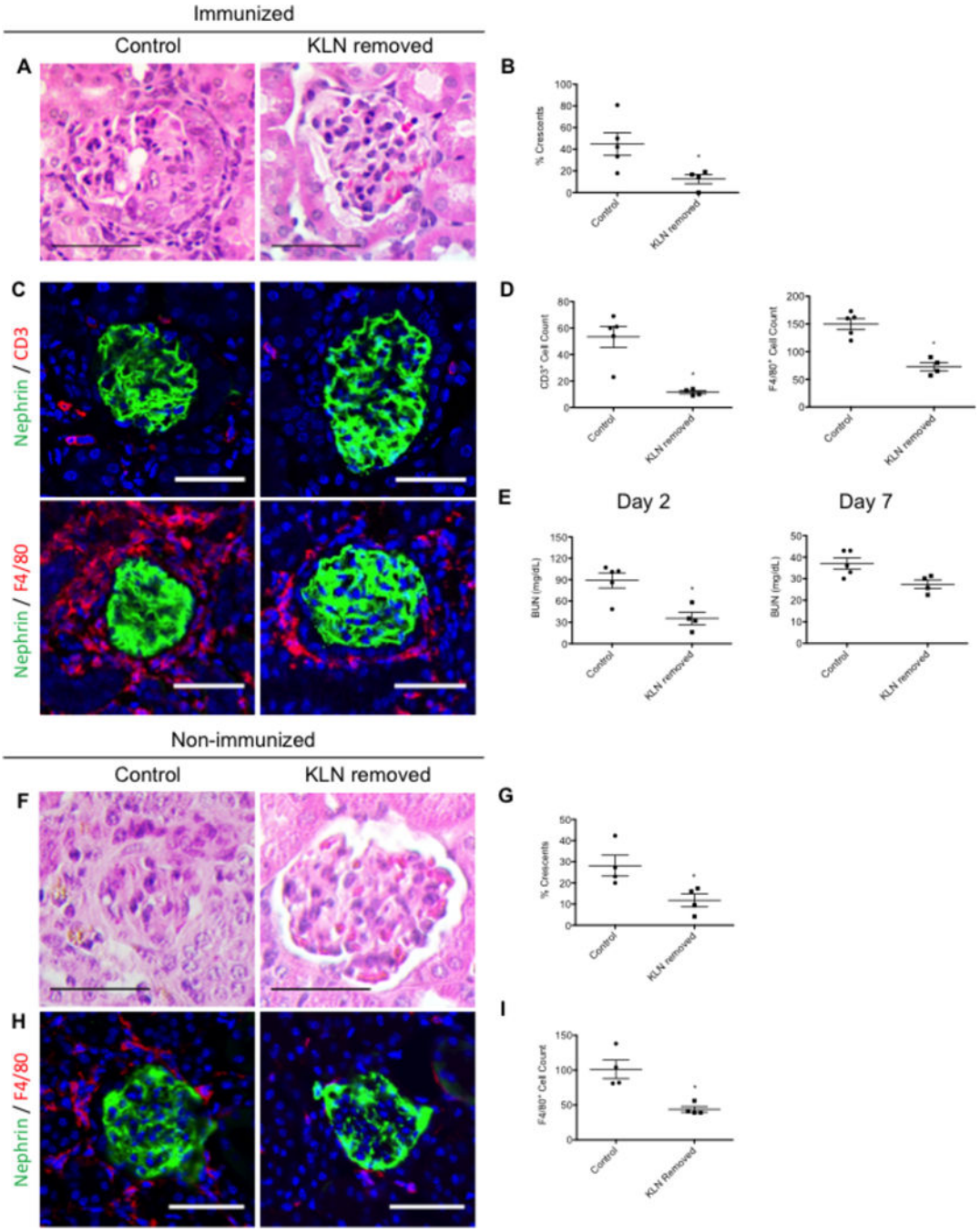

Figure 3. Removal of KLN results in protection from kidney injury in NTN.

(A) Representative figure of H&E stained kidney at NTN Day 7 shows glomerulus with crescent in control mouse that underwent sham surgery and normal appearance of glomerulus in kidney of mouse following KLN removal. Scale bar 50 μm. **(B)** Percentage of crescentic glomeruli in kidneys at Day 7 decreases following KLN removal (Control: n=5, mean 44.96%±10.44, range 17.85714–80.76923%, median 42.85714%; KLN removed: n=4, 12.5%±4.279, 0– 19.04762%, median 15.476205%). **(C)** Infiltration of $CD3^+$ T cells (red, top row) and $F4/80^+$ macrophages (red, bottom row) decreases in kidney following KLN

removal Glomerulus marker nephrin (green), nuclear marker DAPI (blue). Scale bar 50 μm. **(D)** $CD3^+$ and $F4/80^+$ cell counts decrease following KLN removal ($CD3^+$ T cells: Control: *n*=5, 53.4±7.966, 23–69, median 60; KLN removed: *n*=4, 11.5±1.19, 9–14, median 11.5) ($F4/80^+$ macrophages: Control: *n*=5, 149.8 ±9.82, 120–173, median 160; KLN removed: *n*=4, 73±7.405, 57–90, median 72.5). **(E)** BUN at Days 2 and 7 is reduced in mice following KLN removal (Day 2: Control: *n*=5, 88.91±10.68, 48.57907–107, median 101; KLN removed: *n*=4, 35.5±8.649, 16.137360–58.14828, median 33.853445) (Day 7: Control: *n*=5, 37±2.627, 30–43,median 36; KLN removed: *n*=4, 27.43±2.028, 22.54018–31.32203, median 27.93848) (*p*=0.0635 for Day 7). **(F)** Glomerulus with crescent in control mouse that underwent sham surgery and normal appearance of glomerulus in kidney of mouse following KLN removal in the absence of pre-immunization. (**G**) In the non-immunized NTN model, the percentage of crescentic glomeruli in kidneys at Week 3 decreases following KLN removal (Control: *n*=4, 28.16%±4.9444, 20–42.30769%, median 25.174825; KLN removed: *n*=4, 11.77%±3.06, 4.166667 17.391300%, median 6.845238%). (**H**) Infiltration of $F4/80^+$ macrophages (red) decreases in kidney following KLN removal in the absence of pre-immunization at Day 3. Glomerulus marker nephrin (green), nuclear marker DAPI (blue). Scale bar 50 μm. (**I**) $F4/80^+$ macrophage cell counts decrease following KLN removal in the absence of pre-immunization at Day 3 (Control: *n*=4, 101.3±13.35, 81–138, median 121; KLN removed: *n*=4, 43.75±4.11, 39–56, median 47.5). *$p<0.05$. KLN: kidney lymph node, NTN: nephrotoxic serum nephritis, H&E: hematoxylin and eosin, BUN: blood urea nitrogen. Data in graphs are presented as means (horizontal bar) ± SEM (vertical bars).

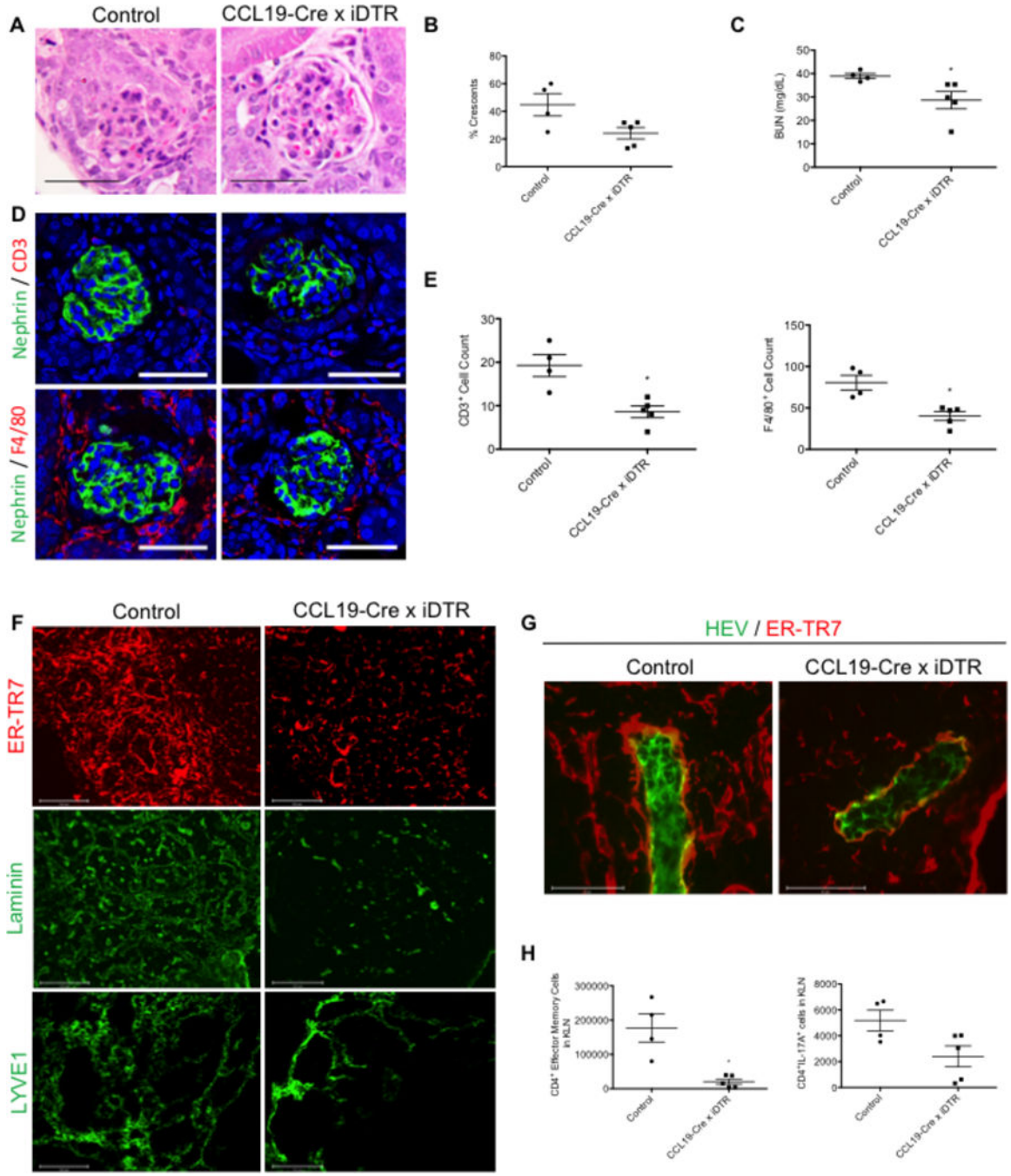

Figure 4. FRC depletion results in protection from kidney injury in NTN.

(A) Glomerulus with crescent in C57Bl/6 mouse (control) and normal appearance of glomerulus in kidney of CCL19-Cre x iDTR mouse in NTN following FRC depletion (H&E). Scale bar 50 μm. **(B)** Percentage of crescentic glomeruli in kidneys at Day 7 decreases following FRC depletion (Control: n=4, mean 44.75%±8.057, range 25–60%, median 47.008545%; CCL19-Cre x iDTR: n=5, 24.14%±4.127, 13.33333–32%, median 28.57143%) (p=0.1111). **(C)** BUN at Day 7 is significantly reduced in mice following FRC depletion (Control: n=4, 38.95±1.109, 36.51896–41.79039, median 38.750875; CCL19-Cre

x iDTR: n=5, 28.66±3.7, 15.1556–35.33628, median 29.75764) **(D)** Immunohistochemistry of kidney shows decreased infiltration of $CD3^+$ T cells (red, top row) and $F4/80^+$ macrophages (red, bottom row) in kidney in CCL19-Cre x iDTR kidney, as reflected by cell count quantification in **(E)** ($CD3^+$ T cells: Control: n=4, 19.25±2.529, 13–25, median 19.5; CCL19-Cre x iDTR: n=5, 8.6±1.327, 4–12, median 9) ($F4/80^+$ macrophages: Control: n=4, 80.5±8.78, 63–98, median 80.5; CCL19-Cre x iDTR: n=5, 40.2±5.352, 22–50, median 47). Glomerulus marker nephrin (green), nuclear marker DAPI (blue). Scale bar 50 μm. **(F)** FRC depletion results in decreased deposition of ER-$TR7^+$ (red) fibers, reduced laminin fiber (green) formation, and decreased invasion of $LYVE1^+$ lymphatic endothelial cells (green). Scale bar 100 μm. (**G)** FRC depletion results in decreased density of ER-$TR7^+$ fibers (red) surrounding $PNAd^+$ HEV (green), which contains fewer pockets. Scale bar 50 μm. (**H**) $CD4^+$ effector memory cell ($CD4^+CD44^{high}CD62L^{low}$) and Th17 ($CD4^+IL\text{-}17A^+$) cell populations decrease in KLN following FRC depletion ($CD4^+$ effector memory cells: Control: n=4, 176993±40796, 80220–267238, median 180256; CCL19-Cre x iDTR: n=5, 20438±7769, 4281–39617, median 15377) (Th17 cells: Control: n=4, 5174±812, 3529–6656, median 5254.5; CCL19-Cre x iDTR: n=5, 2405±808.9, 323–3994, median 3062) (p=0.0635 for Th17 cells). *p<0.05. FRC: fibroblastic reticular cell, NTN: nephrotoxic serum nephritis, H&E: hematoxylin and eosin, BUN: blood urea nitrogen. Data in graphs are presented as means (horizontal bar) ± SEM (vertical bars).

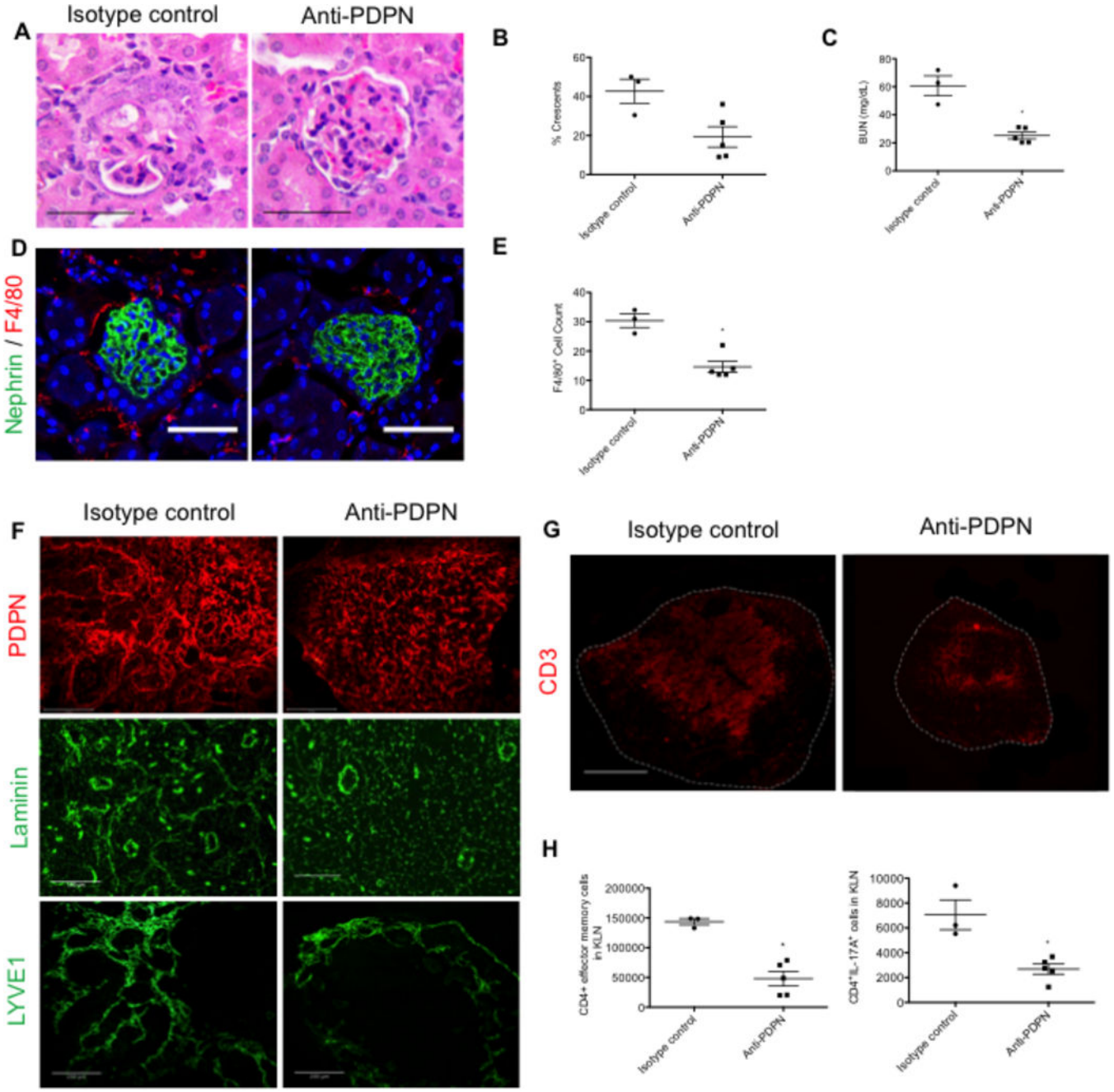

Figure 5. Anti-PDPN treatment results in protection from kidney injury in NTN.

(A) Representative image of H&E stained kidney at NTN Day 7 shows glomerulus with crescent in mouse treated with Syrian hamster IgG (Isotype control) and normal appearance of glomerulus in kidney of mouse treated with anti-PDPN. Scale bar 50 μm. **(B)** Percentage of crescentic glomeruli in kidneys at Day 7 decreases following anti-PDPN treatment (Isotype Control: n=3, mean 42.68%±6.163, range 30.43478–50%, median 47.61905%; Anti-PDPN: n=5, mean 19.26%±5.251, 9.090909–36%, median 15%) (p=0.0714). **(C)** BUN at Day 2 is significantly reduced in mice following anti-PDPN treatment (Isotype Control: n=3, 60.7±7.141, 47.42062–71.88976, median 62.79528; Anti-PDPN: n=5, 25.2±2.407,

20.33778–31.1811, median 23.35867) **(D)** Immunohistochemistry of kidney shows decreased infiltration of F4/80^{+} macrophages (red) in kidney at Day 7, as reflected by cell count in (**E**) (Isotype Control: n=3, 30.33±2.333, 26–34, median 31; Anti-PDPN: n=5, 14.6±1.887, 12–22, median 13). Glomerular marker nephrin (green), nuclear marker DAPI (blue). Scale bar 50 μm. **(F)** Following anti-PDPN treatment, lattice-like pattern of PDPN^{+} (red) cell staining is absent, laminin fibers (green) are less organized and thinner, and LYVE1^{+} lymphatic endothelial cells (green) remain confined to the periphery of the KLN. Scale bars μm for PDPN, 100 μm for laminin, 200 μm for LYVE1. **(G)** CD3^{+} (red) T cell zone is reduced in size following anti-PDPN treatment. Scale bar 500 μm. (**H**) CD4^{+} effector memory cell (CD4^{+}CD44^{high}CD62L^{low}) (Isotype Control: n=3, 143525±5188, 133158–149084, median 148334; Anti-PDPN: n=5, 47871±12277, 20134–78970, median 48816) and Th17 (CD4^{+}IL-17A^{+}) cell populations (Isotype control: n=3, 7052±1194, 5533–9406, median 6216; Anti-PDPN: n=5, 2684±412.4, 1243–3675, median 2746) decrease in KLN following anti-PDPN treatment. *p<0.05. PDPN: podoplanin, anti-PDPN: anti-podoplanin antibody,H&E: hematoxylin and eosin, NTN: nephrotoxic serum nephritis. KLN: kidney lymph node. Data in graphs are presented as means (horizontal bar) ± SEM (vertical bars).